JACS
JOURNAL OF THE AMERICAN CHEMICAL SOCIETY

Article

pubs.acs.org/JACS

Self-Sorting in the Formation of Metal–Organic Nanotubes: A Crucial Role of 2D Cooperative Interactions

Maiko Obana,[†] Takahiro Fukino,*[,†] Takaaki Hikima,[‡] and Takuzo Aida*[,†,§]

[†]School of Engineering, The University of Tokyo, 7-3-1 Hongo, Bunkyo-ku, Tokyo 113-8656, Japan
[‡]RIKEN SPring-8 Center, 1-1-1 Kouto, Sayo-cho, Sayo-gun, Hyogo 679-5148, Japan
[§]RIKEN Center for Emergent Matter Science, 2-1 Hirosawa, Wako, Saitama 351-0198, Japan

Supporting Information

ABSTRACT: A mixture of ferrocene-based tetratopic pyridyl ligands **FcL1** and **FcL2** undergoes self-sorting upon competitive coordination with $AgBF_4$, affording homomeric nanotubes **FcNT1** and **FcNT2** as a mixture. No mutual interference for the nanotubular growth occurred between **FcNT1** and **FcNT2** even when one of these ligands was used in large excess with respect to the other. 2D X-ray diffraction analysis of unidirectionally oriented nanotube samples, prepared by using the capillary technique, revealed that although **FcL1** as reported previously stacks helically in the resulting nanotube **FcNT1** **FcL2** prefers to stack with no discernible helical twist in **FcNT2**. Such a difference in their stacking geometries is most likely a major reason for why mixed-ligand metal–organic nanotubes are not constructed upon competitive coordination of **FcL1** and **FcL2** with $AgBF_4$.

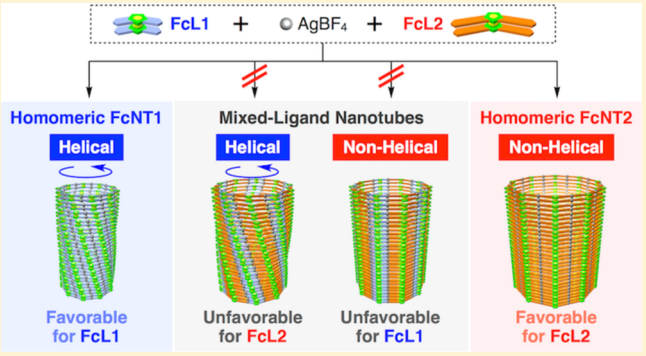

INTRODUCTION

Not only covalent nanotubes such as carbon nanotubes but also noncovalent ones just as those highlighted in this article are potentially useful as tailor-made unidirectional transporters for both mass and energy at the nanoscale and have attracted great attention.[1−4] Although nanotubes adopt a 1D shape morphologically, the assembling mechanism is complicated in comparison with those for 1D solid fibers[5] because nanotubes in reality are a rolled-up 2D assembly where both longitudinal and lateral interactions among adjacent monomers are supposed to operate in a highly cooperative manner (Figure 1). In this regard, the behaviors of microtubules, which are representative biological nanotubular objects, are known to be modulated by cooperation of longitudinal and lateral interactions.[6] However, for synthetic noncovalent nanotubes, such a cooperative nature as expected for self-assembled 2D objects has barely been investigated so far.

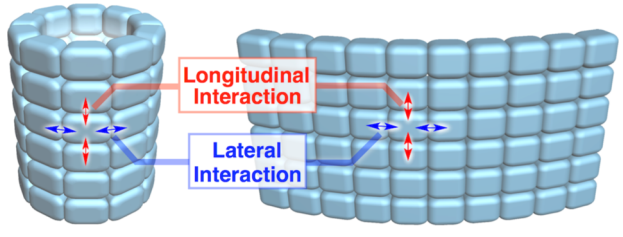

Figure 1. Schematic representations of a self-assembled nanotube (left) and its developed view (right). Nanotubes adopt a 1D shape but, in reality, are composed of a rolled-up 2D assembly, where both of longitudinal and lateral interactions among constituent monomer units operate in a highly cooperative manner.

Recently, we reported that ferrocene (Fc)-based tetratopic pyridyl ligands **FcL1** and **FcL2** (Figure 2) which are designed to be floppy on account of their rotational freedom at the central Fc module assemble upon coordination with $AgBF_4$ into metal–organic nanotubes **FcNT1** and **FcNT2**, respectively.[4a] These nanotubes are composed of uniaxially stacked decagonal nanorings comprising 10 Fc ligands and 20 Ag(I) ions. A detailed study revealed that the nanotubes are constructed stochastically without preceding nanoring formation. Then, we came to wonder if one may possibly diversify the structures of the metal–organic nanotubes by competitive coordination of **FcL1** and **FcL2** with $AgBF_4$. As reported below, we found by using model ligands that the binding affinities of **FcL1** and **FcL2** toward Ag(I) are nearly comparable to one another. As shown in Figure 3b, one can draw seven mixed-ligand nanorings with a planar, decagonal geometry from **FcL1** and **FcL2**, so we envisioned that coassembled nanotubes with such mixed-ligand nanorings as fundamental constituents would indeed form if no mutual interference occurs between **FcL1** and **FcL2**. However, contrary to our expectation, no coassembly between **FcL1** and **FcL2** took place, but only their homomeric nanotubes formed as a mixture. Self-sorting is an entropically disfavored event. This particular molecular

Received: May 6, 2016
Published: June 30, 2016

DOI: 10.1021/jacs.6b04693
J. Am. Chem. Soc. 2016, 138, 9246−9250

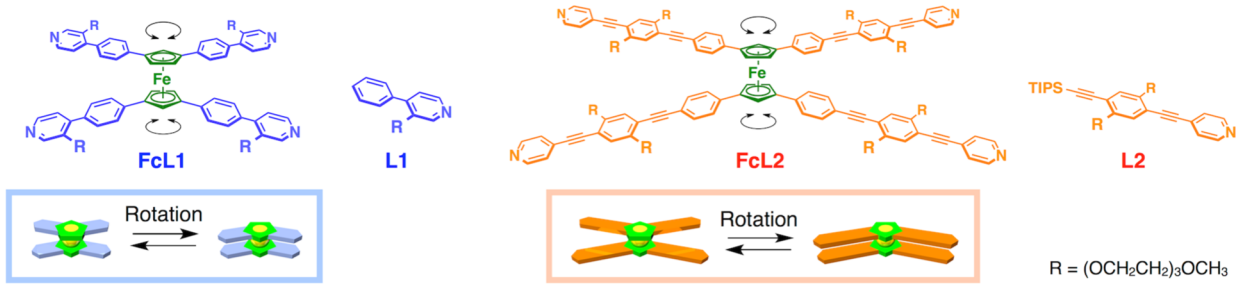

Figure 2. Schematic molecular structures of tetratopic pyridyl ligands **FcL1** and **FcL2** and monotopic pyridyl ligands **L1** and **L2**.

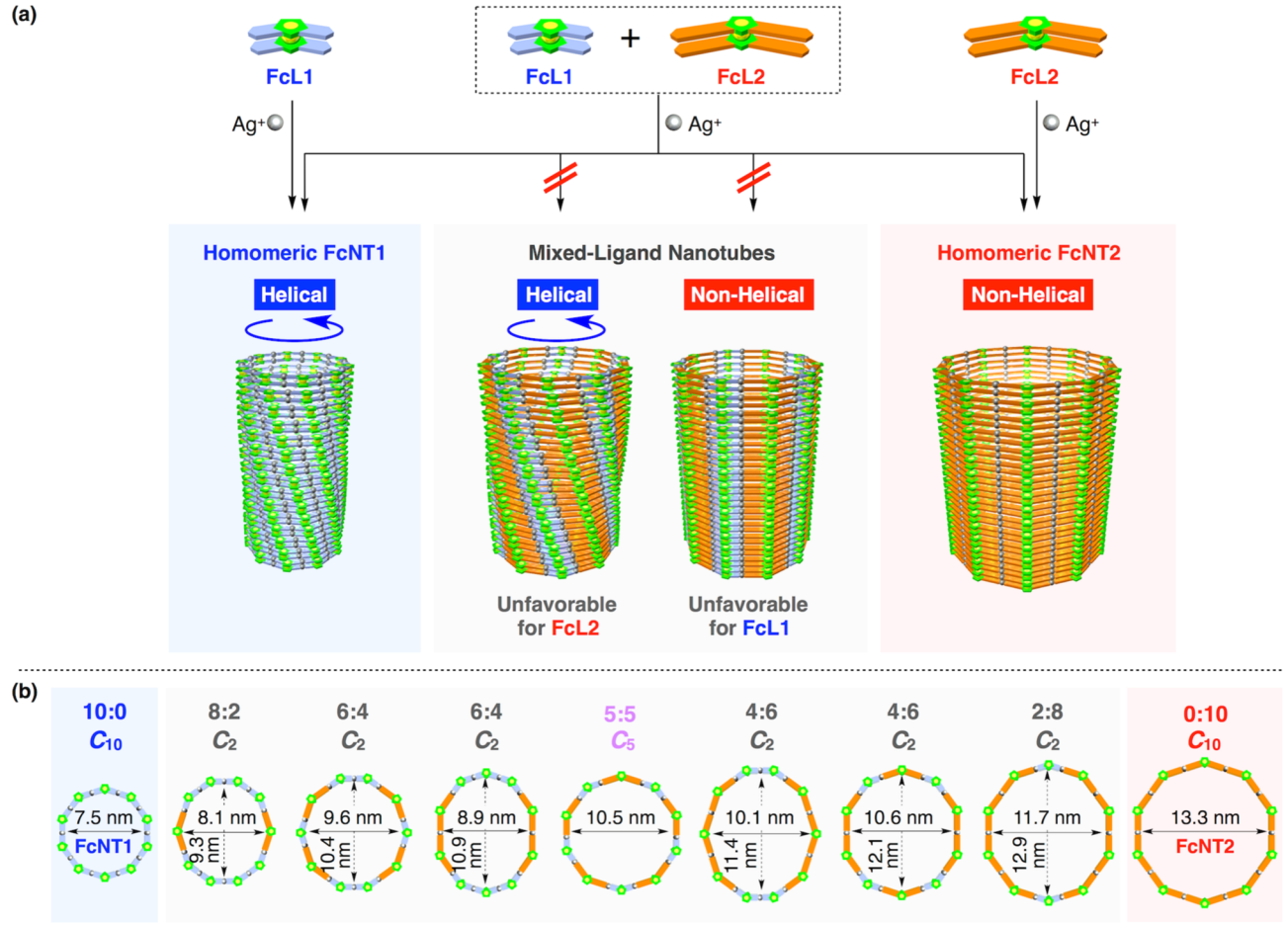

Figure 3. Schematic representations of (a) homomeric metal−organic nanotubes **FcNT1** and **FcNT2** and mixed-ligand nanotubes and (b) decagonal cross sections of possible nanotubes. As for the term "non-helical", see ref 13.

recognition has been investigated in a wide variety of self-assembling systems.[7−9] However, in the nanotubular assembly, no successful example except chiral self-sorting[3] has been reported before the present work. Self-sorting other than chiral self-sorting is called "general self-sorting",[8b] where the size and shape of monomers as "major molecular codes", including the number, orientation, and spatial arrangement of their principal interacting groups, have been understood to determine the assembling pathway, whereas chiral self-sorting makes an issue of other molecular codes such as the complementarity of interactions.[8b] If individual monomers carry considerably different major molecular codes from one another and give assembled objects of different shapes, then general self-sorting is likely to occur even when multiple different monomers are used.[7c] However, if their major molecular codes are not largely different, then prediction of the assembling pathway still remains a big challenge.[9] For these reasons, to explore why **FcL1** and **FcL2** are self-sorted is of general importance in molecular assembly and recognition. As reported herein, it is most likely that self-sorting of **FcL1** and **FcL2** (Figure 3a) is mainly caused by the difference in their preferred stacking angles.

RESULTS AND DISCUSSION

We conducted ^{1}H NMR spectral titration of **L1** (Figure 2), a monotopic model ligand for **FcL1**, with $AgBF_4$ in CD_3CN at 23 °C (Figure 4). Although the spectral features were rather dynamic, we successfully obtained association constants (K_a) for 1:1 $[Ag(\mathbf{L1})]^+$ (K_a = 32 ± 12 M^{-1}) and 1:2 $[Ag(\mathbf{L1})_2]^+$ (K_a = (10.9 ± 6.3) × 10^2 M^{-2}) complexes (Figure 4a) by means of

DOI: 10.1021/jacs.6b04693
J. Am. Chem. Soc. 2016, 138, 9246−9250

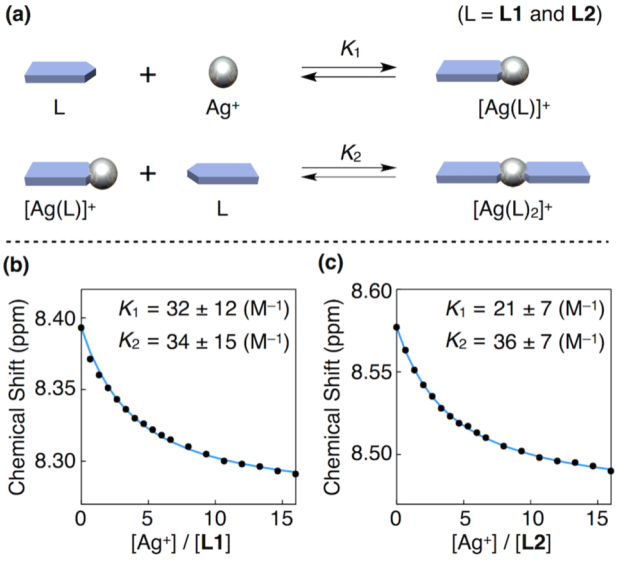

Figure 4. (a) Schematic representations of the coordination equilibria between L, Ag^+, $[Ag(L)]^+$, and $[Ag(L)_2]^+$ (L = **L1** or **L2**). (b and c) Changes in chemical shifts of the signals due to α-protons of the pyridyl units in **L1** (b; 5 mM) and **L2** (c; 10 mM) upon titration with $AgBF_4$ in CD_3CN at 23 °C (black dots), together with their fitting profiles (cyan curves).

nonlinear curve fitting using the WinEQNMR2 program (Figure 4b).[10] Likewise, the K_a values for 1:1 $[Ag(\mathbf{L2})]^+$ (K_a = 21 ± 7 M^{-1}) and 1:2 $[Ag(\mathbf{L2})_2]^+$ (K_a = (7.6 ± 2.9) × 10^2 M^{-2}) complexes (Figure 4a) were obtained (Figure 4c). The results indicate that the K_a values for $[Ag(\mathbf{L2})]^+$ and $[Ag(\mathbf{L2})_2]^+$ differ only marginally from those for $[Ag(\mathbf{L1})]^+$ and $[Ag(\mathbf{L1})_2]^+$, respectively. Hence, it is likely that the intrinsic binding affinities of **FcL1** and **FcL2** toward Ag(I) in the nanotubular assembly are comparable to one another.

Figure 3b shows seven mixed-ligand decagonal nanorings possibly drawn with **FcL1** and **FcL2**. All of these nanorings adopt a planar geometry and could potentially serve as fundamental constituents for coassembled metal−organic nanotubes. Note that the C_2- and C_5-symmetric mixed-ligand nanorings for example are estimated to emerge with 5- and 2-times higher probabilities than the corresponding C_{10}-symmetric homomeric nanorings (Figure S6).[11] The fact that **FcL1** and **FcL2** have nearly comparable binding affinities toward Ag(I) (*vide ante*) is also a positive factor for their coassembly if they do not interfere with one another. However, only homomeric **FcNT1** and **FcNT2** formed (Figure 3a). As a typical example, $AgBF_4$ (20 mM) was added to an MeCN solution of a mixture of **FcL1** and **FcL2** ([**FcL1**] = [**FcL2**] = 5.0 mM), and the resulting mixture was allowed to stand at 25 °C without stirring. After 24 h, an aliquot of the assembling mixture was taken out, diluted with water/EtOH (4:1, v/v), and then negatively stained with uranyl acetate. As shown in Figure 5a, transmission electron microscopy (TEM) after air-drying successfully visualized long nanotubes (length > 500 nm) with two different diameters (wall center-to-wall center distances) of 7 and 13 nm, which are in excellent agreement with the calculated diameters of **FcNT1** (7.5 nm) and **FcNT2** (13.3 nm), respectively (Figure 3b).[4a]

Small-angle X-ray scattering (SAXS) analysis of the assembling mixture of **FcL1** and **FcL2** in MeCN with $AgBF_4$ showed a nonperiodic oscillatory pattern (Figure 5b, green), which is substantially the same as the superimposed image

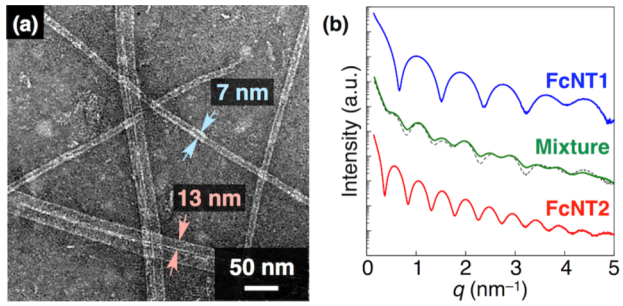

Figure 5. (a) TEM image of an air-dried MeCN/EtOH/water dispersion of an assembled mixture of **FcL1**, **FcL2**, and $AgBF_4$ in MeCN ([**FcL1**] = [**FcL2**] = 5.0 mM; [$AgBF_4$] = 20 mM). The sample was negatively stained with uranyl acetate. For a lower-magnification image, see Figure S4.[11] (b) SAXS profiles of MeCN dispersions of **FcNT1** ([**FcL1**] = 5.0 mM; [$AgBF_4$] = 10 mM; blue), **FcNT2** ([**FcL2**] = 5.0 mM; [$AgBF_4$] = 10 mM; red), and an assembled mixture of **FcL1** (5.0 mM), **FcL2** (5.0 mM), and $AgBF_4$ (20 mM) at 20 °C (green). The broken curve represents a superimposed image of the blue and red curves. For clarity, the blue and red curves are offset by a factor of 10^3 and 10^{-3}, respectively.

(Figure 5b, black dashed) of the SAXS patterns of **FcNT1** (Figure 5b, blue) and **FcNT2** (Figure 5b, red) separately prepared. Even when one of two ligands was used in large excess (3:1) with respect to the other, the nanotubular products did not lose their structural and compositional integrities (Figure S3).[11] Therefore, we conclude that a mixture of **FcL1** and **FcL2**, upon competitive coordination with $AgBF_4$, undergoes self-sorting to give only homomeric nanotubes **FcNT1** and **FcNT2** as a mixture (Figure 3a). The fact that neither mutual interference between **FcL1** and **FcL2** in their homomeric nanotubular growth nor coassembly of **FcL1** and **FcL2** into mixed-ligand nanotubes takes place was a big surprise to us, considering that these ligands possibly compete with one another in the binding toward Ag(I).

We noticed that the stacking geometry of **FcL2** is different from that of **FcL1**, i.e., **FcL2** prefers to stack up with no discernible helical twist whereas **FcL1** stacks helically in **FcNT1** as reported in our previous paper.[4b] For investigating the assembling geometries, 2D XRD analysis of oriented samples is effective. Thus, similar to the case of **FcNT1**,[4] we applied a 10 T magnetic field to an MeCN dispersion of **FcNT2** under conditions for slow evaporation. However, this method did not work for extra-large-diameter **FcNT2**. After much trial and error, we finally found that the so-called "capillary technique" (Figure S5)[11] allows both **FcNT1** and **FcNT2** to align unidirectionally. **FcNT1** adopts a helical geometry (Figure 3a).[4b] Its oriented sample (counterion = BF_4^-) using the capillary technique (Figure 6a, center) displayed a 2D XRD pattern nearly identical to that of the magnetically oriented sample (counterion = a mixture of $CF_3SO_3^-$ and BF_4^-) reported in our previous paper.[4] Most characteristic were multiple sets of four-split diffraction spots at q = 4.08 nm^{-1} (d = 1.54 nm; purple arrows), 7.66 nm^{-1} (d = 0.82 nm; gray arrows), and so forth. Figure 6d (center) shows a 2D XRD pattern of the oriented **FcNT2** sample using the capillary technique. Although this XRD pattern was even better qualified than that of **FcNT1** (Figure 6a, center), it did not show any sign of four-split diffraction spots characteristic of helical structures. The absence of such a characteristic feature in the 2D XRD pattern of **FcNT2** was more explicitly confirmed by its totally featureless azimuthal plots obtained at q = 4.0−7.0

DOI: 10.1021/jacs.6b04693
J. Am. Chem. Soc. 2016, 138, 9246−9250

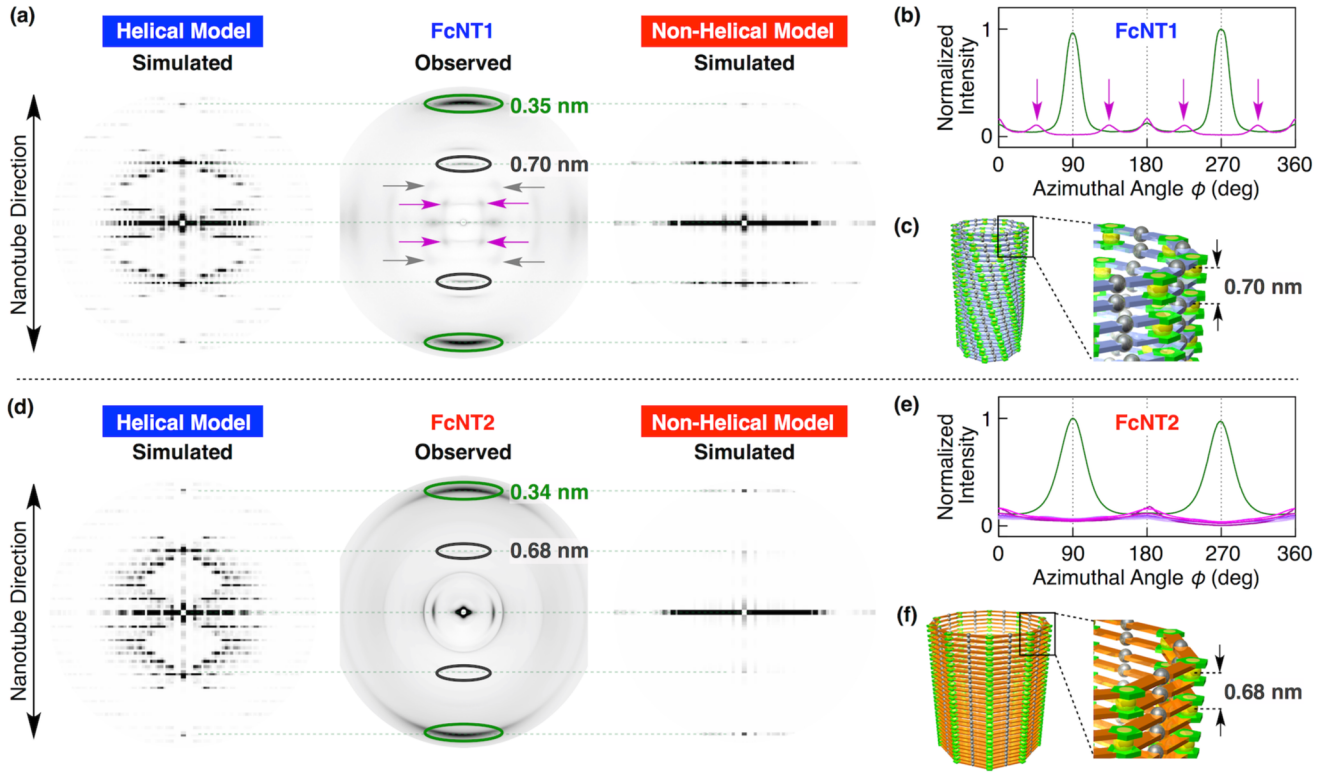

Figure 6. 2D XRD patterns of air-dried MeCN dispersions of (a) **FcNT1** (center; [**FcL1**] = 5.0 mM; [$AgBF_4$] = 10 mM) and (d) **FcNT2** (center; [**FcL2**] = 5.0 mM; [$AgBF_4$] = 10 mM) together with simulated 2D XRD patterns using the HELIX program[12] based on simplified atomistic models for corresponding helical (left) and non-helical (right) nanotubes. Samples of unidirectionally oriented **FcNT1** and **FcNT2** were prepared by using the capillary technique (Figure S5).[11] For parameters used for the simulation, see Table S1.[11] Azimuthal plots for the 2D XRD intensities of **FcNT1** (a, center) at q = 18.0 nm^{-1} (d = 0.35 nm; b, green) and 4.08 nm^{-1} (d = 1.54 nm; b, purple) and those of **FcNT2** (d, center) at q = 18.5 nm^{-1} (d = 0.34; e, green) and 4.0–7.0 nm^{-1} (plotted at every 0.5 nm^{-1}; d = 0.90–1.57 nm; e, purple). Arrows indicate four-split diffraction spots at q = 4.08 nm^{-1} (d = 1.54 nm; purple) and 7.66 nm^{-1} (d = 0.82 nm; gray). Schematic representation of the stacking distances between the constituent nanorings in (c) **FcNT1** and (f) **FcNT2**.

nm^{-1} (d = 0.90–1.57 nm; Figure 6e, purple). In sharp contrast, the azimuthal plot for the 2D XRD pattern of **FcNT1** displayed a set of explicit peaks at q = 4.08 nm^{-1} (d = 1.54 nm), corresponding to the four-split diffraction spots (Figure 6b, purple). By using the HELIX program,[12] we generated simulated 2D XRD patterns for non-helical (Figure 6d, right) and helical (Figure 6d, left) nanotubular models and confirmed that the former resembles the actual 2D XRD pattern of **FcNT2** (Figure 6d, center) but the latter does not. These results allow us to conclude that **FcL2** in **FcNT2** stacks up with no discernible helical twist (Figure 3a). We consider that the helical geometry of **FcNT1** is possibly induced by a propeller-chiral geometry at its aromatic arm parts.[4b] In contrast, the aromatic units in the arm parts of **FcL2** can be coplanarized through an ethynyl linker and would therefore have no steric bias toward the propeller chirality. Note that a non-helical geometry of **FcNT2**[13] possibly allows for the operation of a Ag(I)–Ag(I) metallophilic interaction between adjacent metal–organic nanorings.[4a,14]

Finally, we would like to discuss a possible effect of the stacking distance. If the preferred stacking distance of **FcL2** is different from that of **FcL1**, then these ligands would not coassemble into a single nanotube. The 2D XRD patterns of **FcNT1** and **FcNT2** (Figure 6) are also informative to this issue and actually indicated that the stacking distance of **FcL1** in **FcNT1** (0.70 nm, Figure 6c) is only 0.02 nm larger than that of **FcL2** in **FcNT2** (0.68 nm, Figure 6f). Obviously, this difference is too small to explain why **FcL1** and **FcL2** are self-sorted. On the basis of all the experimental results, we now conclude that the observed self-sorting is mainly due to the different stacking geometries between **FcL1** and **FcL2** upon nanotubular assembly (Figure 3a).

■ CONCLUSIONS

In the present study, we found a 2D cooperative nature in the nanotubular assembly of **FcL1** and **FcL2** with $AgBF_4$ under competitive conditions. If the assembled product is a simple metal–organic 1D chain, then the use of two ligands such as **FcL1** and **FcL2** with comparable affinities toward Ag(I) would obviously result in the formation of mixed-ligand 1D sequences. However, in the nanotubular assembly **FcL1** and **FcL2** were self-sorted (Figure 3a), affording a mixture of homomeric **FcNT1** and **FcNT2**. Once again, nanotubes in reality are a rolled-up 2D assembly, where both of longitudinal and lateral interactions among adjacent monomer units operate in a highly cooperative manner (Figure 1). Hence, as highlighted in the present work, two tube-forming monomers, even though they are analogous in major molecular codes to one another,[8] would not form mixed-ligand nanotubes, if they have different preferences for the stacking geometry such as the stacking angle. Our metal–organic nanotubes are composed of uniaxially stacked nanorings[4] but do not consist of helically assembled 1D chains that are more frequently seen in literatures. Such a structural feature is very rare but quite

DOI: 10.1021/jacs.6b04693
J. Am. Chem. Soc. 2016, 138, 9246–9250

advantageous for exploring how 2D cooperative interactions among constituent monomers are essential in the molecular assembly. We believe that the obtained rationale is important for diversifying and elaborating nanoscale molecular objects.

■ ASSOCIATED CONTENT

Supporting Information

The Supporting Information is available free of charge on the ACS Publications website at DOI: 10.1021/jacs.6b04693.

Details of synthesis; analytical data obtained by ^{1}H and ^{13}C NMR, TEM, and SAXS (PDF)

■ AUTHOR INFORMATION

Corresponding Authors

*fukino@macro.t.u-tokyo.ac.jp

*aida@macro.t.u-tokyo.ac.jp

Notes

The authors declare no competing financial interest.

■ ACKNOWLEDGMENTS

This work was supported by the Japan Society for the Promotion of Science (JSPS) through a grant-in-aid of Specially Promoted Research (25000005) on "Physically Perturbed Assembly for Tailoring High-Performance Soft Materials with Controlled Macroscopic Structural Anisotropy", as well as by the "Nanotechnology Platform" program (12024046) of the Japanese Ministry of Education, Culture, Sports, Science, and Technology (MEXT). Synchrotron radiation experiments were performed at the BL45XU[15] beamline of SPring-8 with the approval of the RIKEN SPring-8 Center (proposal 20150022). We thank V. K.-M. Au, J. Bergueiro, P. K. Hashim, and E. S. Silver for fruitful discussion.

■ REFERENCES

(1) Selected reviews on self-assembled nanotubes: (a) Kameta, N.; Minamikawa, H.; Masuda, M. *Soft Matter* **2011**, *7*, 4539. (b) Chapman, R.; Danial, M.; Koh, M. L.; Jolliffe, K. A.; Perrier, S. *Chem. Soc. Rev.* **2012**, *41*, 6023. (c) Barclay, T. G.; Constantopoulos, K.; Matisons, J. *Chem. Rev.* **2014**, *114*, 10217.

(2) Selected examples of self-assembled nanotubes: (a) Ghadiri, M. R.; Granja, J. R.; Milligan, R. A.; McRee, D. E.; Khazanovich, N. *Nature* **1993**, *366*, 324. (b) Hill, J. P.; Jin, W.; Kosaka, A.; Fukushima, T.; Ichihara, H.; Shimomura, T.; Ito, K.; Hashizume, T.; Ishii, N.; Aida, T. *Science* **2004**, *304*, 1481. (c) Jin, W.; Fukushima, T.; Niki, M.; Kosaka, A.; Ishii, N.; Aida, T. *Proc. Natl. Acad. Sci. U. S. A.* **2005**, *102*, 10801. (d) Johnson, R. S.; Yamazaki, T.; Kovalenko, A.; Fenniri, H. *J. Am. Chem. Soc.* **2007**, *129*, 5735. (e) Yamamoto, T.; Fukushima, T.; Kosaka, A.; Jin, W.; Yamamoto, Y.; Ishii, N.; Aida, T. *Angew. Chem., Int. Ed.* **2008**, *47*, 1672. (f) Tu, S.; Kim, S. H.; Joseph, J.; Modarelli, D. A.; Parquette, J. R. *J. Am. Chem. Soc.* **2011**, *133*, 19125. (g) Zhang, W.; Jin, W.; Fukushima, T.; Saeki, A.; Seki, S.; Aida, T. *Science* **2011**, *334*, 340. (h) Yagai, S.; Yamauchi, M.; Kobayashi, A.; Karatsu, T.; Kitamura, A.; Ohba, T.; Kikkawa, Y. *J. Am. Chem. Soc.* **2012**, *134*, 18205. (i) Huang, Z.; Kang, S.-K.; Banno, M.; Yamaguchi, T.; Lee, D.; Seok, C.; Yashima, E.; Lee, M. *Science* **2012**, *337*, 1521. (j) Eisele, D. M.; Cone, C. W.; Bloemsma, E. A.; Vlaming, S. M.; van der Kwaak, C. G. F.; Silbey, R. J.; Bawendi, M. G.; Knoester, J.; Rabe, J. P.; Vanden Bout, D. A. *Nat. Chem.* **2012**, *4*, 655. (k) Zhang, W.; Jin, W.; Fukushima, T.; Mori, T.; Aida, T. *J. Am. Chem. Soc.* **2015**, *137*, 13792.

(3) Examples of chiral self-sorting in nanotubular assembly: (a) Sato, K.; Itoh, Y.; Aida, T. *Chem. Sci.* **2014**, *5*, 136. (b) Pantoş, G. D.; Wietor, J.-L.; Sanders, J. K. M. *Angew. Chem., Int. Ed.* **2007**, *46*, 2238.

(4) (a) Fukino, T.; Joo, H.; Hisada, Y.; Obana, M.; Yamagishi, Y.; Hikima, T.; Takata, M.; Fujita, N.; Aida, T. *Science* **2014**, *344*, 499. (b) Yamagishi, H.; Fukino, T.; Hashizume, D.; Mori, T.; Inoue, Y.; Hikima, T.; Takata, M.; Aida, T. *J. Am. Chem. Soc.* **2015**, *137*, 7628.

(5) A review on the assembling mechanisms: Zhao, D.; Moore, J. S. *Org. Biomol. Chem.* **2003**, *1*, 3471.

(6) (a) Frieden, C. *Annu. Rev. Biophys. Biophys. Chem.* **1985**, *14*, 189. (b) Huber, F.; Schnauß, J.; Rönicke, S.; Rauch, P.; Müller, K.; Fütterer, C.; Käs, J. *Adv. Phys.* **2013**, *62*, 1.

(7) Pioneering works on self-sorting: (a) Krämer, R.; Lehn, J.-M.; Marquis-Rigault, A. *Proc. Natl. Acad. Sci. U. S. A.* **1993**, *90*, 5394. (b) Taylor, P. N.; Anderson, H. L. *J. Am. Chem. Soc.* **1999**, *121*, 11538. (c) Wu, A.; Isaacs, L. *J. Am. Chem. Soc.* **2003**, *125*, 4831. (d) Addicott, C.; Das, N.; Stang, P. J. *Inorg. Chem.* **2004**, *43*, 5335.

(8) Selected reviews on self-sorting: (a) Northrop, B. H.; Zheng, Y.-R.; Chi, K.-W.; Stang, P. J. *Acc. Chem. Res.* **2009**, *42*, 1554. (b) Safont-Sempere, M. M.; Fernández, G.; Würthner, F. *Chem. Rev.* **2011**, *111*, 5784. (c) Lal Saha, M.; Schmittel, M. *Org. Biomol. Chem.* **2012**, *10*, 4651. (d) He, Z.; Jiang, W.; Schalley, C. A. *Chem. Soc. Rev.* **2015**, *44*, 779.

(9) Selected examples of self-sorting: (a) Morris, K. L.; Chen, L.; Raeburn, J.; Sellick, O. R.; Cotanda, P.; Paul, A.; Griffiths, P. C.; King, S. M.; O'Reilly, R. K.; Serpell, L. C.; Adams, D. J. *Nat. Commun.* **2013**, *4*, 1480. (b) Saha, M. L.; Schmittel, M. *J. Am. Chem. Soc.* **2013**, *135*, 17743. (c) Ayme, J.-F.; Beves, J. E.; Campbell, C. J.; Leigh, D. A. *Angew. Chem., Int. Ed.* **2014**, *53*, 7823. (d) Jiménez, A.; Bilbeisi, R. A.; Ronson, T. K.; Zarra, S.; Woodhead, C.; Nitschke, J. R. *Angew. Chem., Int. Ed.* **2014**, *53*, 4556. (e) Klotzbach, S.; Beuerle, F. *Angew. Chem., Int. Ed.* **2015**, *54*, 10356. (f) Fu, J.-H.; Lee, Y.-H.; He, Y.-J.; Chan, Y.-T. *Angew. Chem., Int. Ed.* **2015**, *54*, 6231.

(10) Hynes, M. J. *J. Chem. Soc., Dalton Trans.* **1993**, 311.

(11) See Supporting Information.

(12) Knupp, C.; Squire, J. M. *J. Appl. Crystallogr.* **2004**, *37*, 832.

(13) The term "non-helical geometry" neither means that the stacking angle is exactly zero degrees nor guarantees the absence of any macroscopic helical structure.

(14) A review on Ag(I)−Ag(I) metallophilic interaction: Khlobystov, A. N.; Blake, A. J.; Champness, N. R.; Lemenovskii, D. A.; Majouga, A. G.; Zyk, N. V.; Schröder, M. *Coord. Chem. Rev.* **2001**, *222*, 155.

(15) Fujisawa, T.; Inoue, K.; Oka, T.; Iwamoto, H.; Uruga, T.; Kumasaka, T.; Inoko, Y.; Yagi, N.; Yamamoto, M.; Ueki, T. *J. Appl. Crystallogr.* **2000**, *33*, 797.

DOI: 10.1021/jacs.6b04693
J. Am. Chem. Soc. 2016, 138, 9246−9250